Accuracy Improvement in the Nano-displacement Measurement Based on the Doppler-Interferometry Method by Cross-talk Reduction

Saeed Olyaee   **Shahram Mohammad Nejad**

Optoelectronic and Laser Laboratory, Department of Electrical Engineering,
Iran University of Science and Technology (IUST)

s_olyaee@srttu.edu   shahramm@iust.ac.ir

Abstract

In this paper, accuracy improvement in the displacement measurement systems using Doppler-interferometry method is presented. The cross-talk error reduction methods are also discussed. Based on the mentioned method, a new nano-displacement measurement system is designed. In the designed system, the signal to leakage ratio for moving targets in the range of -20m/s to +20m/s is increased to 55dB. The measured phase detection error is equal to 7.9 degree in the normal condition, and after the cross-talk error reduction it is reduced to 0.11 degree. As a result, the displacement measurement error is decreased from 6.9nm to 0.1nm.

Keywords: cross-talk error, Doppler-interferometry, nano-displacement, He-Ne laser.

1- Introduction

In optical instruments such as laser interferometer, various parameters affect the accuracy. The error sources in the laser interferometer systems include the non-linearity in the optical section, intensity fluctuation and laser frequency instability, environment turbulences, misalignment in the optical instruments, systematic error in the phase detection, and cross-talk error. Several error sources are considered as linear errors that can be simply reduced or eliminated [1-3]. But the cross-talk error especially in the heterodyne method produces the non-linearity error. This effect on the laser range finders based on the phase shift method is reported in [4].

Heterodyne methods such as Doppler-interferometry compared to homodyne methods provide more signal to noise ratio and easy alignment. Because of using the two separated beams in the heterodyne method, the non-linearity errors especially cross-talk error is dominance [5-7]. By combining the reference and the measurement fields, the phase error is obtained from

$$\Phi_{err} = \theta_o - \Phi_o = \tan^{-1}\left(-I_{ol} / I_{ot}\right) \qquad (1)$$

where θ_o is the measurement phase, Φ_o is the real phase, I_{ot} and I_{ol} are the main signal and leakage amplitudes, respectively. The diagram of the main signal I_{ot}, leakage I_{ol}, and the measurement signal I_{om} in the heterodyne system is shown in figure 1. The amplitude of the measurement signal is given by

$$I_{om} = \sqrt{I_{ol}^2 + I_{ot}^2 + 2I_{ol}I_{ot}\cos\Phi_{err}} \qquad (2)$$

According to Eq.2 and figure 1, the phase error and hence the systematic errors will increase by increasing the leakage amplitude.
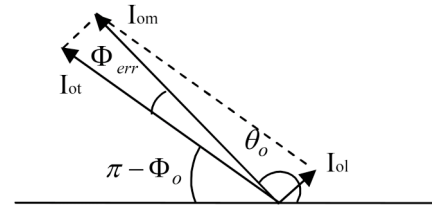

Fig.1: Diagram of the main signal, leakage, and measurement signal in the heterodyne system.

2- Cross-talk error in the Doppler-interferometer

Two main sources produce the cross-talk error in the laser Doppler-interferometer. The first one includes the electrical induction between the reference and measurement paths. The other one is due to the unwanted electromagnetic leakage of two modes. The output beam contains two orthogonal linearly components with small difference between their frequencies. As a result, the laser output can be used as a reference beam and measurement beam, separately. Ideally a polarizing beam splitter (PBS) can separate the laser output into two beams with different wavelengths and polarizations. But, in practical systems, there exist a non-orthogonality between the linear beam polarization and elliptical polarization of the individual beams. And hence, after separation, a small fraction of each mode is available in the other.

Figure 2 shows the block diagram of the velocity and nano-displacement measurement system based on the laser Doppler-interferometry. The current to voltage converter (IVC), pre-amplifier, and comparator circuits are similar in the K_1 and K_2 boxes.
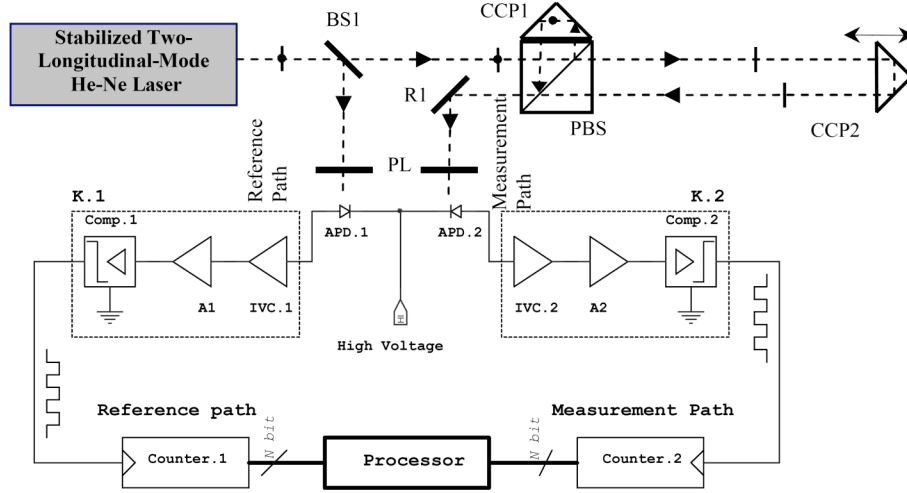
Fig. 2: Block diagram of the velocity and nano-displacement measurement system. BS: beam splitter, PBS: polarizing beam splitter, CCP1: corner cube prism1 (reference) and CCP2: corner cube prism2 (target).
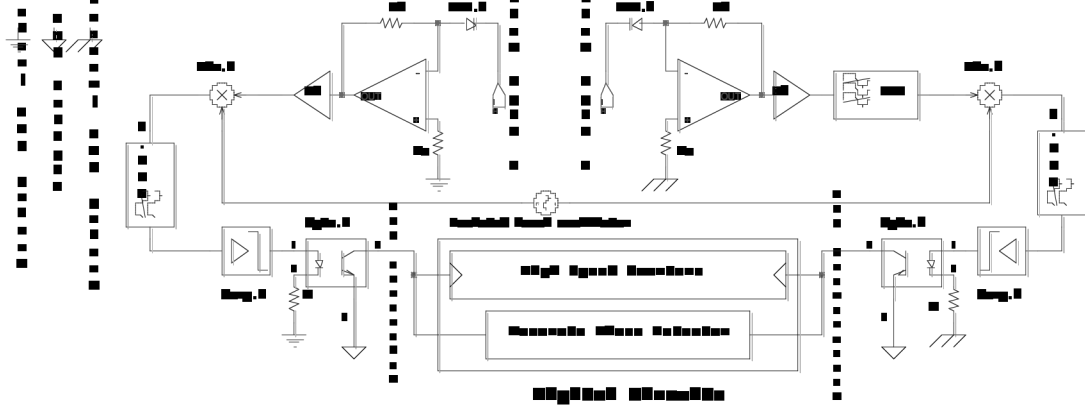

Fig. 3: Schematic diagram of the electronic section of the velocity and nano-displacement measurement system with noise and cross-talk error reduction.

The photocurrent of the APD at the measurement path (APD_2) is given by

$$I_{APD_2} = k[E_1 \cos(2\pi v_1 t) + E_2 \cos(2\pi v'_2 t + \varphi + \Phi)]^2 \quad (3)$$

where v_1 and v_2 are the frequencies of two modes $(v_o = v_2 - v_1)$, ϕ is the initial phase between the two, Φ is the phase shift due to difference in the optical paths, and v'_2 is the reflected beam frequency of the target mirror (CCP_2). The reflected beam frequency is obtained as

$$v'_2 = v_2 \pm 2n\overline{V} / \lambda_2 \quad (4)$$

where $\overline{V}$ is the velocity of the target and n is the refractive index of the medium along the laser path.

Considering the cross-talk error, a fraction of reference mode (with v_1 frequency) includes in the measurement mode. The leakage frequency, therefore, is shifted by an amount $\pm 2n\overline{V} / \lambda_1$, $(v'_1 = v_1 \pm 2n\overline{V} / \lambda_1)$. As mentioned above, the leakage amplitude is much smaller than the main signal amplitude $(\widetilde{E}_1 << E_1)$. Hence, the photocurrent of avalanche photodiode (Eq.3) is corrected as

$$I'_{APD_2} = k\begin{bmatrix} E_1 \cos(2\pi v_1 t) + \widetilde{E}_1 \cos(2\pi v'_1 t + \Phi) \\ + E_2 \cos(2\pi v'_2 t + \varphi + \Phi) \end{bmatrix}^2 \quad (5)$$

In addition, the high frequencies are eliminated by APD_2. As a result, the Eqs.3 and 5 are simplified to

$$I_{APD_2} = 2kE_1 E_2 \cos(2\pi(v_o \pm 2n\overline{V} / \lambda_2) + \varphi + \Phi(t)) \quad (6)$$

$$I'_{APD_2} = 2kE_1\widetilde{E}_1 \cos(2\pi(\pm 2n\overline{V} / \lambda_1) + \Phi(t)) +$$
$$+ 2kE_1 E_2 \cos(2\pi(v_o \pm 2n\overline{V} / \lambda_2) + \varphi + \Phi(t)) + \quad (7)$$
$$+ 2k\widetilde{E}_1 E_2 \cos(2\pi(v_o \pm 2n\overline{V}(1/\lambda_2 - 1/\lambda_1)) + \varphi)$$

In Eq.7, the first and third terms are the cross-talk components and the second term (similarly to Eq.6) is the main signal. The last term can be rewritten as $2k\widetilde{E}_1 E_2 \cos(2\pi v_o(1 \pm 2n\overline{V} / C) + \varphi)$, where $|v_2 - v_1| / C$ is equal to inverse of the synthetic wavelength, λ_s.

3- The cross-talk error reduction method

As is shown in figure 2, a stabilized two-longitudinal-mode He-Ne laser having 632.8nm wavelength and 152MHz free spectral range is used. Therefore, the maximum measurable velocity is equal to $\overline{V}_{\max} = \lambda v_o / 2n = 48.1 m/s$. By approaching the target (CCP_2) close to the system, for example with $1 m/s$ velocity, the frequencies of Eq.7 are obtained as 3.16MHz, 155.16MHz, and 152MHz, respectively.

The schematic diagram of the electronic section of the velocity and nano-displacement measurement system with noise and cross-talk error reduction techniques is shown in figure 3. The analog ground (including reference and measurement grounds) and digital ground are isolated. Also, two isolated high voltage power supplies are used for APD biasing.
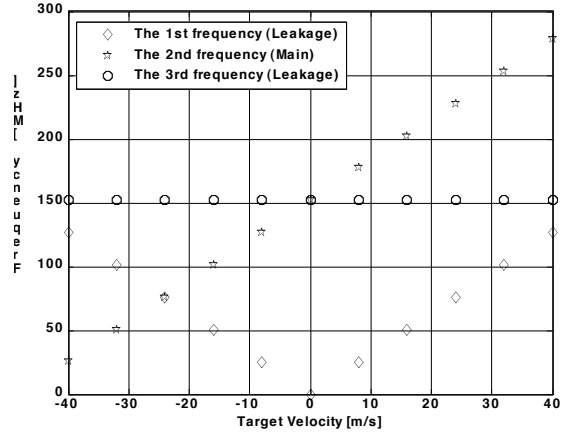

Fig.4: The measurement frequencies (main and leakage) in terms of the target velocity.

The measurement frequencies in terms of the target velocity is shown in figure 4. By using a band pass filter (BPF) having cut-off frequencies equal to 75MHz and 230MHz, the leakage signal is considerably reduced. Although, the maximum measurable velocity is limited to $\pm 20 m/s$, but the cross talk error is reduced dramatically. The input and output signals of the measurement band pass filter (BPF) is shown in figure 5. The output signal of the measurement BPF is mixed with the local oscillator signal ($f_l = 233 MHz$). The new frequencies in terms of the target velocity is shown in figure 6 (the bold line is the main signal frequency, the dashed lines are the leakage frequencies, and the dotted line is the image frequency). The amplitude of the measurement signal for velocities $\pm 20 m/s$ and $\pm 5 m/s$ is shown in figure 7. The leakage and image frequencies are finally eliminated by a low pass filter whose cut-off

frequency is 150MHz. The output signals of the LPFs passed through opto-coupler isolators and exerted to digital section. In this section, an accurate phase detector measured the initial and final phases between the reference and measurement signals. Also, a high speed counter measured the shifted frequency due to the Doppler effect. The output of counter 1 is proportional to the free spectral range of the laser (the frequency difference between the two modes). But the output of counter 2 changes proportional to the speed of the target. Comparing the counter's outputs, the direction is detected.
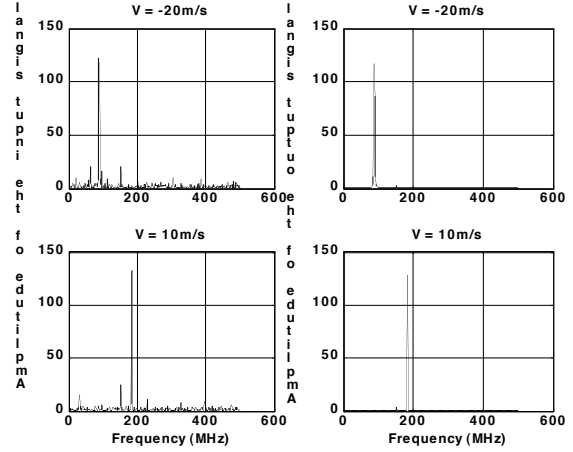

Fig.5: Left- the input and right- the output signals of the measurement band pass filter (BPF).
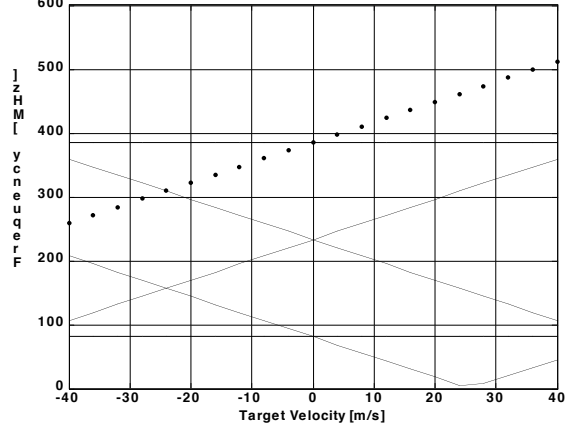

Fig.6: The output frequencies of the measurement mixer (Mix.2) in terms of the target velocity. The bold line is the main signal frequency, the dashed lines are the leakage frequencies, and the dotted line is the image frequency.

4- Results

In this system the cross-talk error is reduced by,

i. Coupling reduction between reference and measurement paths by using a proper shielding, grounding and using the two isolated power supplies.

ii. Noise reduction by using an electromagnetic interference shield.

iii. Laser power reduction.
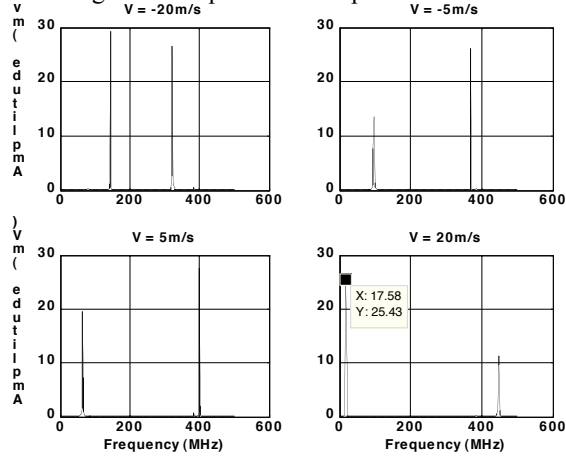
iv. Using the band pass and low pass filters.

Fig.7: The amplitude of the measurement signals after the noise and cross-talk reduction ($\pm 20 m/s$ and $\pm 5 m/s$).

The measurement signal amplitude and phase detection error in terms of leakage amplitude is depicted in figure 8. In the normal condition, the amplitude of the main signal and total leakage are 398.7mV and 55.3mV, respectively. As a result, according to Eq.8, the signal to leakage ratio (SLR) is increased considerably, and is given by

$$ SLR = I_{ot} / \left(\sum_{i=1}^{n} I^2_{ol_i} \right)^{1/2} \qquad (8) $$

where I_{ot} is the main signal amplitude and I_{ol_i} is the amplitude of the ith leakage. Based on the mentioned methods, the signal to leakage ratio is reached to 55dB. The displacement resolution is obtained as

$$ \Delta d = \frac{\lambda}{2} \left(N + \left(\Phi_2 - \Phi_1 \right) / 2\pi \right) \qquad (9) $$
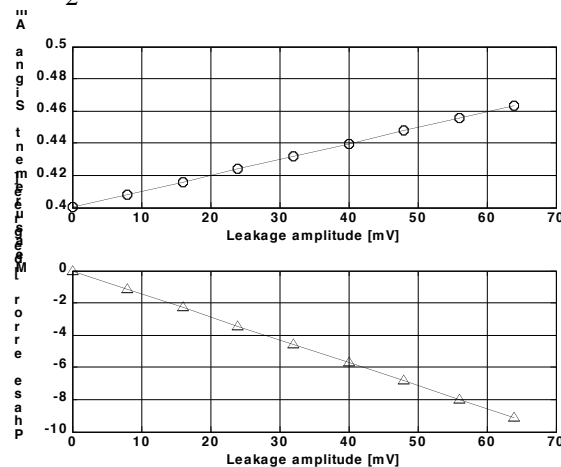

Fig.8: The measurement signal amplitude and phase detection error in terms of leakage amplitude.

where λ is the central wavelength, N is the shifted frequency due to the Doppler effect, Φ_1 and Φ_2 are

the initial and final phases between the reference and measurement signals, respectively. Since the detected phase is changed by leakage, so the error in the nanometric displacement measurement $\left(\delta_d \right)$ is expressed as

$$ \delta_d = \frac{\lambda}{2} \left[\tan^{-1} \left(I_{ol} / I_{ot} \right) / 2\pi \right] \qquad (10) $$

The phase detection error before and after the noise and cross-talk reduction are 7.9 and 0.11 degree, respectively. The displacement error is limited to 0.1nm; despite the fact that it was 6.9nm before the cross-talk error reduction. The summary of the designed system's performances is described in table.1.

Table.1: The summary of the typical performance.

Parameter	Before the noise and cross-talk reduction	After the noise and cross-talk reduction
Main signal amplitude	398.7mV	441.3mV
Total leakage amplitude	55.3mV	0.81mV
SLR	17dB	55dB
Phase detection error	7.9^o	0.11^o
Displacement error	6.9nm	0.1nm

5. References

[1] J.F. Meyers, J. W. Lee and R. J. Schwartz, "Characterization of measurement error sources in Doppler global velocimetry", *Meas. Sci. Technol.* 12, 357–368, 2001.

[2] Sutton C M, "Nonlinearity in the length measurement using heterodyne laser Michelson interferometry", *J. Phys. E: Sci. Instrum.* 20 1290–2, 1987.

[3] Hou W and Wilkening G, "Investigation and compensation of the nonlinearity of heterodyne interferometers", *Prec. Eng.* 14 91–8, 1992.

[4] S.Mohammad Nejad and S.Olyaee , "Cross-Talk and Intermediate Frequency Deviation Effects on Phase-Shift Range Finder", *Iranian Journal of Science and Technology, Vol.26, No.B4,* PP. 647-654, 2002.

[5] Patterson S and Beckwith J, "Reduction of systematic errors in heterodyne interferometric displacement measurement", *Proc. 8th IPES Conf. (Compiegne, France)* pp 101–4, 1995.

[6] Rosenbluth A E and Bobroff N, "Optical sources of nonlinearity in heterodyne interferometers", *Precision Eng.* 12 7–11, 1990.

[7] T.Eom, T.Y.Choi, K.Lee, H.Choi and S.Lee, "A simple method for the compensation of the nonlinearity in the heterodyne interferometer", *Meas. Sci. Technol.* 13, 222–225, 2002.